Impact of Spatial and Spectral Granularity on the Performance of SDM Networks Based on Spatial Superchannel Switching

Behnam Shariati, *Student Member, IEEE*, José Manuel Rivas-Moscoso, Dan M. Marom, *Fellow, OSA, Senior, IEEE*, Shalva Ben-Ezra, Dimitrios Klonidis, Luis Velasco, Ioannis Tomkos, *Fellow, OSA, Senior, IEEE*

***Abstract*—Spatially integrated switching architectures have been recently investigated in an attempt to provide switching capability for networks based on spatial division multiplexing (SDM) fibers, as well as to reduce the implementation cost. These architectures rely on the following switching paradigms, furnishing different degrees of spectral and spatial switching granularity: *independent switching* (Ind-Sw), which offers full spatial-spectral flexibility; *joint-switching* (J-Sw), which treats all spatial modes as a single entity; and *fractional-joint switching* (FrJ-Sw), whereby sub-groups of spatial modes are switched together as independent units. The last two paradigms are categorized as *spatial group switching* (SG-Sw) solutions since the spatial resources (modes, cores, or single-mode fibers) are switched in groups. In this paper, we compare the performance (in terms of spectral utilization, data occupancy, and network switching infrastructure cost) of the SDM switching paradigms listed above for varying spatial and spectral switching granularities in a network planning scenario. The spatial granularity is related to the grouping of the spatial resources, whereas the spectral granularity depends on the channel baud rate and the spectral resolution supported by wavelength selective switches (WSS). We consider two WSS technologies for handling of the SDM switching paradigms: 1) the current WSS realization, 2) WSS technology with a factor-two resolution improvement. Bundles of single-mode fibers are assumed across all links as a near-term SDM solution. Results show that the performance of all switching paradigms converge as the size of the traffic demands increases, but finer spatial and spectral granularity can lead to significant performance improvement for small traffic demands. Additionally, we demonstrate that spectral switching granularity must be adaptable with respect to the size of the traffic in order to have a globally optimum spectrum utilization in an SDM network. Finally, we calculate the number of required WSSs and their port count for each of the switching architectures under evaluation, and estimate the switching-related cost of an SDM network, assuming the current WSS realization as well as the improved resolution WSS technology.**

***Index Terms*—SDM networks, superchannel switching, spatial and spectral granularity, WSS**

I. Introduction

THE continuous increase in the amount of data originating from online applications and services has led to an unremitting 20-60% annual traffic growth in telecommunication networks [1]. The most immediate consequence of this is that transmission requirements are inexorably approaching the capacity limit of the single-mode fibre (SMF) [2]. A way forward would be the use of space division multiplexing (SDM) over multi-core fibers (MCF), multi-mode fibers (MMF), few-mode multi-core fibers (FM-MCF), or even bundles of SMFs, which would allow the network capacity to scale to orders of magnitude higher than what can be achieved with an SMF-based network infrastructure [2] [3], while reducing the cost per bit delivered to the end users by sharing network elements among different spatial dimensions (e.g. integration of multiple optical switching elements [5][4], integration of transceivers to form a spatial super-channel (Sp-Ch) [6], or integration of optical amplifiers [7][8]). Note, however, that the selection of a cost-effective technology for each element of an SDM network may result in the introduction of additional physical-layer constraints that need to be taken into account [4][9][10].

Thus far, SDM research has mainly focused on SDM fiber technology and transmission performance [11][12][13]. The extra physical impairments introduced by SDM media (compared to the case of SMF transmission) have been thoroughly investigated [10], e.g., MCF is mostly affected by inter-core crosstalk (XT), while MMF is strongly impacted by mode coupling and/or differential mode delay. For the purpose of our study, SDM media can be categorized in three groups, according to whether they have 1) uncoupled/weakly-coupled spatial dimensions (cores, modes or parallel fibers), 2) strongly coupled spatial dimensions, or 3) sub-groups of strongly coupled spatial dimensions [4]. The choice of a transmission medium belonging to one or another of these three categories is a key factor in determining the required architecture and

Manuscript received September 26, 2015; accepted …….; published ….. (Doc. ID ……..). This work was supported by the European Commission's Seventh Framework Program FP7/2012-2015 through the INSPACE project under grant agreement n. 619732 (http://www.ict- inspace.eu) the Spanish MINECO SYNERGY project (TEC2014-59995-R).

B. Shariati is with Athens Information Technology (AIT), Marousi 15125, Athens, Greece and Universitat Politécnica de Catalunya (UPC), Barcelona 08034, Spain. (e-mail: b.shariati@ait.gr).
J. M. Rivas-Moscoso, D. Klonidis, and I. Tomkos are with AIT,
D. M. Marom is with Hebrew University of Jerusalem, Jerusalem, Israel.
S. Ben-Ezra is with Opsys Technologies, Holon, Israel.
L. Velasco is with UPC.

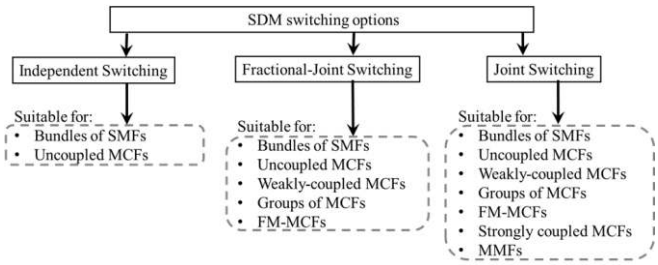

Fig. 1. Classification of SDM switching paradigms and suitable transmission media for each category.

TABLE I
VALUES OF SELECTED CHBW WITH THE AMOUNT OF CORRESPONDING SPECTRAL CONTENTS SUPPORTED BY TWO WSS TECHNOLOGIES

Spectral Channel plan [GHz]	50	43.75	37.5	31.25	25
Current generation WSS resolution (clear channel BW and % utilization)	32	25.75	19.5	13.25	7
	64%	59%	52%	42%	28%
Improved resolution WSS technology (clear channel BW and % utilization)	41	34.75	28.5	22.25	16
	82%	79%	76%	71%	64%

properties of the optical switches at the nodes of an SDM-based network [14]. For instance, strongly coupled MCFs or MMFs necessitate that all cores/modes be switched together as the information is in a mixed state, whereas, at the opposite extreme, the use of bundles of SMFs permits both independent and joint switching of the signals on each of the SMFs. A middle-ground solution, e.g. FM-MCF with negligible coupling between cores, would allow independent switching of the mode groups on each of the cores (with a small reach penalty due to the existing, though small, inter-core XT) or joint switching of all modes/cores. Therefore, switching strategies can be divided into several paradigms which strongly correlate with the SDM fiber categories defined above [4][5]: (a) *independent switching* (Ind-Sw), whereby all spectral slices and spatial dimensions can be independently directed to any output port; (b) *joint switching* (J-Sw), in which all S spatial dimensions (S is the number of core/modes per SDM fiber) are treated as a single entity, while spectral slices can still be independently switched; and (c) *fractional joint switching* (FrJ-Sw), a hybrid approach in which a number of subgroups of G spatial dimensions out of S ($G>1$), as well as all spectral slices, can be independently switched to all output ports. The last two paradigms can be categorized as *spatial group switching* (SG-Sw) solutions since the spatial resources are switched in groups rather than independently, as in the case of Ind-Sw. Note that several *spatial switching granularities* result from different levels of grouping of the spatial dimensions: from G=1, which assumes individual fibers, thus corresponding to the Ind-Sw case and offering the finest spatial granularity, all the way through to $G = S$, which considers all spatial dimensions as one spatial group, thus corresponding to the J-Sw case and offering the coarsest spatial granularity. A list of compatible transmission media for each switching paradigm is shown in Fig. 1.

In planning an SDM network, the choice of one of the above SDM switching paradigms has a considerable impact on both the flexibility of the implemented resource allocation (RA) policies [19] and the switching infrastructure deployment cost. For instance, Ind-Sw brings a high level of flexibility for routing, space, modulation-level and spectrum assignment (RSMSA) since it allows the allocation of demands over different spatial dimensions and spectral slices with variable widths [20], but it increases the complexity of the switching architecture, and hence the cost. In contrast, in J-Sw the complexity of the switches is reduced to the SMF equivalent, but the spectrum assignment is limited to a single connection across all spatial dimensions within a spectral slice, with the consequent drawback that the unused spatial dimensions at a certain spectral slot cannot be allocated to other demands.

Two RA policies were explored in [21][22]: *spectral* and *spatial* superchannel (Sp-Ch) allocation. A spectral Sp-Ch is the result of aggregating signals modulated on adjacent optical carriers in a single spatial dimension. A spatial Sp-Ch, on the other hand, results from the aggregation of signals modulated on a certain optical carrier across a number or all of the spatial dimensions of an SDM transmission medium. A third possible policy would emerge from the combination of the aforementioned spectral and spatial allocation options.

In this paper, we investigate the impact of *spatial switching granularity* and *spectral switching granularity* on the performance and the implementation cost of spatial Sp-Ch switching schemes. We only consider the spatial Sp-Ch allocation policy because: (i) it permits comparing all SDM switching paradigms (ii) it allows decreasing the optical switching complexity, since channels are switched in groups (i.e. Sp-Chs) rather than independently —at the price, of course, of a potential reduction in routing flexibility— [22]; and (iii) SDM networks based on spatial Sp-Ch allocation can benefit from additional cost reduction due to the possibility of sharing network elements among different spatial dimensions (e.g., a number of Sp-Ch constituents can share lasers and digital signal processing (DSP) modules, which can lead to cost and power consumption savings of integrated transceivers in SDM networks [27][28][29]).

The paper is structured as follows. In section II, we put the proposed study into context by reviewing related work and highlighting the novelty of the paper. A detailed description of the SDM switching technologies and our cost model for the switching infrastructure, centered on the case in which bundles of SMFs are used as transmission medium, is presented in section III. The simulation environment and assumptions are explained in section IV. Section V is in turn dedicated to the network performance results (and related discussions) and the switching infrastructure cost analysis, respectively. Finally, in section VI, we present our conclusions.

II. RELATED WORK AND NOVELTY OF THE PAPER

Several works have dealt with networking level performance evaluations of SDM networks and, in particular, resource allocation strategies. In [23], a routing, spectrum and core assignment (RSCA) algorithm was proposed aiming at minimizing the spectrum utilization in a weakly-coupled MCF-based SDM network. The problem was formulated as an integer linear programming and a heuristic algorithm was proposed. In [24], considering the spectral Sp-Ch allocation policy, the authors extended the RSCA algorithm presented in [23] to

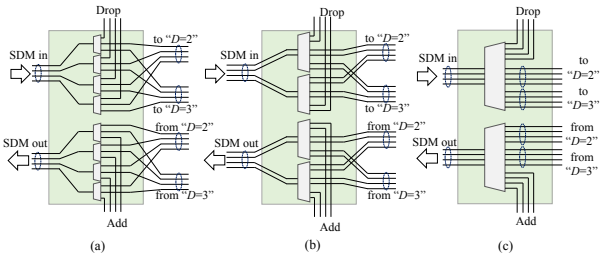

Fig. 2. Interface to one direction of an SDM ROADM node, for S=4 and D=3, enabling a) Ind-Sw (without spatial lane changes), b) FrJ-Sw with G=2, and c) J-Sw. Only 1 degree is shown. Ind-Sw, FrJ-Sw with G=2, and J-Sw require eight 1×3, four 2×6, and two 4×12 WSSs per degree, respectively.

TABLE II
NUMBER OF WSSS PER DEGREE AND THEIR PORT COUNT FOR DIFFERENT SDM SWITCHING PARADIGMS

switching type	port count per WSS	number of WSS per degree	port count per WSS for bundles of 4 SMFs, G=2, and D=3	number of WSS for bundles of 4 SMFs, G=2 per degree
Ind-Sw	1×D	2.S	(1×3)	8
FrJ-Sw	G×(1×D)	$2\cdot\lceil S/G \rceil$	2×(1×3)	4
J-Sw	S×(1×D)	2	4×(1×3)	2

include the modulation format and jointly optimize the switching and spectrum resource efficiency in weakly-coupled MCF-based SDM networks implemented using architecture on demand and static ROADMs. In [25], routing, spectrum, core, and/or mode assignment methods were proposed which exploited prioritized area concept and XT awareness depending on whether or not MCF or MMF were affected by inter-core/inter-mode XT. Note that the spatial Sp-Ch allocation policy was not investigated in any of these works. In [26], exploiting the spatial Sp-Ch allocation policy, the routing, modulation format, baud rate, and mode assignment problem was addressed with the aim of showing the benefits of FMFs in metro networks. Note that, the two main technology areas limiting channel allocation and routing options in an SDM based optical network are fiber type and switching paradigms. In all said studies, authors made an attempt to address the RA problem with a view to mitigating the impact of the physical layer impairments introduced by SDM fibers (i.e. MCF/MMF). However, the impact of switching paradigms, which determine the routing properties of the multiplexed channel at the SDM nodes, on the performance of SDM networks has not been investigated. The focus of this paper is to compare the performance of the three paradigms described above for switching spatial Sp-Chs considering various spatial and spectral granularities and employing two WSS technologies for their realization. Bundles of SMFs are assumed throughout the study since they permit a fair comparison of Ind-Sw, J-Sw and FrJ-Sw due to the absence of XT between spatial dimensions, as explained above.

Assuming bundles of 12 SMFs, we showed in [15] that the performance of SG-Sw cases becomes similar to that of Ind-Sw as *the total offered load to the network* (hereinafter referred to as *load*) increases, while SG-Sw cases bring up to 50% cost savings compared to the Ind-Sw case. However, SG-Sw cases showed a reduced performance for low values of load. In [16], we further showed that SG-Sw paradigms with lower G values perform well for networks with high level of traffic diversity, while J-Sw is favorable for networks with large demands. In addition, in [17], several algorithms have been proposed to improve the performance of different SDM switching paradigms when uncoupled fibers are in place. Note that in [15][16], Ind-Sw, J-Sw and FrJ-Sw with G = 3 were only examined with a fixed spectral channel width (ChBW) — defined as the spectrum over each of the spatial dimensions used to allocate the spatial Sp-Ch constituents— equal to 50 GHz. In this paper, in addition to the three levels of spatial switching granularity studied in [15][16], we examine FrJ-Sw with G equal to 2, 4, and 6.

The spectral switching granularity is related with the capabilities of *wavelength selective switches* (WSSs). Current WSS technology allows occupying 32-GHz on a 50 GHz grid, which we considered in [15], due to channel pass bandwidth imposed by the WSS resolution. The same WSS resolution can allocate finer channels, typically according to a 6.25 GHz grid, i.e., 25.75 GHz can be provisioned on 43.75 GHz, 19.5 GHz on 37.5 GHz, 13.25 GHz on 31.25, or 7 GHz on 25 GHz. In [18], assuming a ChBW of 50 GHz, 25 GHz, and 12.5 GHz at a baud rate of 32, 16 and 8 Gbaud, respectively, we made an early effort to study the effect of spectral granularity on the performance of SDM switching paradigms. However, WSS technologies with different spectral resolutions were considered for every ChBW-baud rate pair, which impedes a direct comparison of the implementation cost of the required spatial Sp-Ch switches in each case. In this paper, we build on [18] to investigate the impact of the spectral switching granularity on the performance and cost of spatial Sp-Ch switches based on two practical WSS technologies: 1) the current generation WSS realization, 2) a WSS technology with a factor-two resolution improvement (i.e. requiring 9 GHz for guard band instead of the 18 GHz considered above). A summary of the ChBW values selected for this study and the corresponding clear channel bandwidth that can be allocated with data and switched by current and future (factor-two resolution improvement) WSS realizations is provided in Table I. The impact of ChBW and WSS resolution in conjunction with the various switching strategies is investigated in this paper.

III. SDM SWITCHING TECHNOLOGIES

The implementation of switching solutions for the switching paradigms described above requires the design of new SDM switching nodes [4][19]. Ind-Sw can be realized by means of a node architecture such as the one shown in Fig. 2(a) for a route-and-select reconfigurable optical add/drop multiplexer (ROADM) configuration, applicable for transmission fiber without mixing/coupling. It is composed of a number of conventional WSSs, one per spatial dimension, degree and ingress/egress port. Commercially available 1×5, 1×9 or 1×20 WSSs can be employed since the port count is not a limiting factor in this case. The selection of one or another realization will depend on a number of factors, such as the required ROADM operation (e.g. whether "spatial lane change" —i.e. rerouting from one spatial dimension (fiber/core/mode) to another [4]— are allowed) and the nodal degree —i.e. the number of available directions— of the network nodes. Fig. 2(a) depicts a node architecture enabling Ind-Sw without spatial lane change for an SDM network with S = 4 spatial dimensions and a node with degree D = 3. Add/drop modules (not shown in

Fig. 2), depending on the chosen add/drop module/transponder technology, can allow for several degrees of operational flexibility: they can be colorless, directionless and/or contentionless. Colorless, contentionless ROADM architectures were proposed in [4]. Colorless, directionless ROADM architectures were analyzed in [21]. Finally, colorless, directionless, contentionless ROADM architectures are based on multicast switches (MCS) [22][30] or $M\times N$ WSSs [5]. A free-space port-reconfigurable WSS serving as a 7×21 switch was reported in [31]. An 8×28 WSS combining waveguide and free- space optics was demonstrated in [32][33]. In this paper, we assume colorless, directionless and contentionless operation, so that the node architecture depicted in Fig. 2(a) requires two (or four, to avoid a single point of failure) MCSs or $M\times N$ WSSs with 12 input ports and as many output ports as the number of transponders that need aggregating. To relax the requirement of high-port-count (HPC) add/drop modules, K add/drop modules with port count $M\times N/K$ can be used instead, in which case K more output ports per ingress/egress WSS are required.

FrJ-Sw and J-Sw make necessary a redesign of the WSSs. Spatial group (SG) WSSs compatible with bundles of SMF, few-mode fibers (FMF) or MCFs were reported in [28][34][35]. They are configured to operate as $S \times (I \times O)$ WSSs, i.e. they direct I input ports, each carrying S spatial modes/cores, toward O output ports using spatial diversity. In [28], a commercial 1×20 WSS was reconfigured to implement a 7×(1×2) WSS for a 7-core MCF with spatial diversity. In [35], the WSS port count was increased to 57 by replacing the input/output optical frontend with a 2D SMF array laid out in a 19×3 grid. The operation of this HPC WSS as a 6×(1×8) SDM WSS was demonstrated in a heterogeneous SDM network with SMF bundles, FMFs and MCFs. HPC WSS realizations with port count equal to 96, in a 1×(1×95) configuration, was reported in [36], by introducing front-end beam-conditioning optics with a waveguide-based solution acting as a spatial beam transformer (SBT) [37]. Various SDM WSS architectures relying on SBTs were proposed in [38]. Spatial diversity solutions in support of FMFs, MCFs or FM-MCFs, introduce interfaces capable of converting the MCF/FMF inputs/outputs into bundles of SMFs, such as photonic lanterns for FMFs [39] and FM-MCF [40][41], or MCF fan-ins/fan-outs based on 3D direct laser writing [42] or tapered fiber bundles [43] for MCFs, need to be interposed between the fiber and the WSS. Spatial diversity based WSSs suffer from several drawbacks, among them that (i) mode/core demultiplexing and multiplexing before and after each WSS results in excess loss leading to reduced transmission reach, and (ii) the number of output ports to which the S spatial dimensions can be routed is decreased by a factor equal to S. An alternative WSS modification in support of joint switching applicable for the case of FMF transmission is to replace the WSS input/output SMF array with an FMF array. This requires a modification of the anamorphic beam-expansion optics so that the spectral resolving power is increased, thus mitigating the impact of channel bandwidth reduction due to mode dependent loss at channel edges[44]. FMF-WSSs allowing joint switching of three spatial modes in a 3×(1×9) and 3×(1×2) configuration were demonstrated in [44] and [45], respectively.

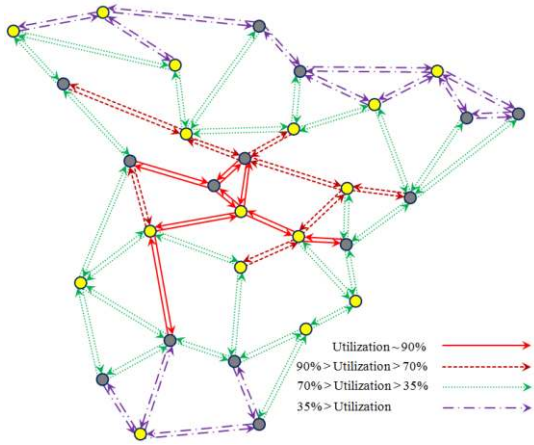

Fig. 3. Topology of Telefónica Spain national network. Nodes with add/drop capabilities are illustrated with filled gray circles. Solid and dashed red lines show the hot links, dotted green lines represent the moderately utilized links, and dashed-dotted purple lines show the underutilized links.

By making use of SG WSSs, the FrJ-Sw and J-Sw paradigms enable reducing the number of necessary WSSs to $2\cdot\lceil S/G\rceil$ and 2, respectively, per degree, as illustrated in Fig. 2(b) and (c), but the required port count increases by a factor of G and S, respectively. In the case of large number of spatial dimensions, the joint-switching paradigm makes it necessary that new realizations be explored. Recently, a technique to increase the port count by implementing a non-trivial unitary transform between an array of Gaussian beams and an array of overlapping Sinc functions (resulting in rectangular shaped beams on the LCoS) has proved to be capable of doubling the WSS port count compared to standard Gaussian illumination [46].

In assessing the strengths and limitations of the three SDM switching paradigms, we must take into account how the architectural complexity of the enabling switching solutions affects, not only the network performance, but also the equipment cost (as will be seen in section V). In particular, as discussed above, cost differences between node architectures will arise from the fact that the required number of WSSs per node and the WSS port count differ according to the chosen switching paradigm (see Table II). In the rest of this section we derive a node cost model for the network switching infrastructure cost analysis in section V. We consider route-and-select node architectures as well as bundles of SMFs as SDM transmission medium, and therefore we focus on WSS realizations with input/output SMF arrays and obviate the need of SDM interfaces. Section V assumes colorless, directionless and contentionless ROADM operation for the network performance, but the cost analysis does not take into account the cost of the add/drop modules since the cost of these modules is strongly dependent on the choice of switching technology (MCS or $M\times N$ WSS), the trade-off between the MCS or $M\times N$ WSS port count and number of units (which also affects the ingress/egress WSS port count, as discussed above), optical amplification needs, and the ratio of *contentionlessly* added/dropped traffic to total traffic.

The node cost model uses the cost of commercial LCoS-based 1×9 WSSs as a reference (cost = 1) and follows the rule that an increase of 4× in the number of ports results in a 2.5× increase in cost, based on a WSS design analysis performed in the framework of the EU project INSPACE [47] and improving

upon a previous HPC WSS cost analysis presented in [15]. Node architectures requiring WSSs with less than 3, 6, 10 and 21 ports (i.e. 1×2, 1×5, 1×9, and 1×20 WSSs, respectively; all commercially available) have a cost per WSS of 0.4, 0.63, 1 and 1.58, respectively. The cost of HPC WSSs with up to 40, 80 and 160 ports (1×40, 1×80, 1×160 WSSs), assuming technology maturity and mass production, was estimated to be 2.50, 3.95, and 6.25, respectively. In [15], the cost per port of the HPC WSSs (>20 ports) was assumed to range between 0.10 and 0.15. These values assumed new product introduction, which explains the higher costs. Likewise, in the present paper (refining the analysis in [15], where a cost per port metric was utilized) we only consider 1×40, 1×80, 1×160 WSSs as HPC WSS realizations since WSSs are introduced in generations. Additionally, we estimate WSSs with improved resolution to be 25% more costly than WSSs with the current optical resolution due to the required optics redesign and larger dispersive elements for enhanced resolution.

IV. Simulation Environment and Assumptions

The network simulations were carried out over the Telefónica Spain national network [48], which is representative of a typical national-scale backbone network in Europe and consists of 30 nodes (average/max. nodal degree 3.7/5). 14 of the nodes are transit nodes with add/drop capabilities and 56 bidirectional links (average length of 148 km). The network is characterized by a symmetric traffic matrix, with 84 connection requests between two subsets of 7 transit nodes, which is significantly heterogeneous. The total amount of traffic (i.e. total amount of all 84 demands) is equal to 10.5 Tb/s estimated for year 2014, when the smallest demand is ~2 Gb/s, the largest one is ~488 Gb/s, and the mean value of all demands is ~125 Gb/s. The heterogeneous nature of the traffic matrix is the consequence of connection requests being mostly exchanged between highly populated transit areas and Madrid/Barcelona (more than 70% of the total traffic flows are from/to Madrid), where the Internet exchange points are located. This leads to the existence of ~30% of *hot links* (i.e. links with more than twice the average spectrum utilization per link in the network), ~20% of *underutilized links* (i.e. links with <1/3 the average spectrum utilization per link in the network) and ~50% of *moderately utilized links*. The topology of Telefónica's network, in which links are differentiated based on their utilization, is shown in Fig. 3.

Even though MCFs/MMFs/FM-MCFs are the ultimate transmission media for SDM networks, to ensure a smooth migration from currently deployed networks to SDM, network operators will seek to leverage their current infrastructure by exploiting the capacity increase enabled by parallel transmission through bundles of SMFs. These have the advantage that the transmission is not affected by XT between spatial dimensions (fibers), and SDM multiplexers/demultiplexers are not required for component interconnection. Assuming bundles of SMFs also allows us to make a fair comparison between different spatial Sp-Ch switching paradigms, due to the fact that the bundles of SMFs are the only type of SDM transmission medium compatible with all switching paradigms.

TABLE III
Maximum point-to-point transmission reach (km) with the indicated baud rate, ChBW, and modulation format

Baud rate in GSamp/s	ChBW in GHz	DP-BPSK	DP-QPSK	DP-8QAM	DP-16QAM
32	50	9800	4900	1900	900
25.75	43.75	10800	5400	2100	1000
19.5	37.5	12300	6100	2400	1200
13.25	31.25	15400	7700	3000	1500
7	25	16650	8300	3250	1650
41	50	7300	3500	1200	600
34.75	43.75	7800	3700	1400	700
28.5	37.5	8300	4000	1500	800
22.25	31.25	9200	4500	1800	900
16	25	10500	5200	2000	1000

We therefore limited the network performance study to the case of bundles of SMFs and implemented a RSMSA algorithm consisting of a diverse routing computation element (a k-fixed —maximum k is 9— alternate shortest path with maximal disjoint links for each source-destination pair [49]) and a resource allocation module in which spatial and spectral resources are assigned to connection requests in the form of spatial Sp-Ch, following a first-fit strategy, starting from the shortest path and the lowest indexed spatial/spectral resource. In order to alleviate the problem posed by the *hot links*, as described above, we implemented a load-balancing engine including a *request-breakdown* element, which breaks up connections larger than the capacity of one spatial Sp-Ch, i.e. the number of SMFs in the bundle. The load-balancing engine distributes big connection requests proportionally over *underutilized* and *moderately utilized* links when the shortest paths between end-nodes become very congested. Obviously, the load-balancing engine is more often used when traffic grows and more alternate shortest paths between source-destination pairs is required to serve one big connection request. Ultimately, the selection of best path and the most adequate spatial/spectral resources to establish a connection is carried out by a simulated annealing meta-heuristic optimization tool equipped with a multi-starting-point generator to avoid local minima, thus yielding a nearly optimal global spectrum utilization [50].

Regarding the transmission technology, single carrier (SC) multi-channel (MC) multi-line rate (MLR) systems [21] were considered, in which the MLR behavior is achieved by changing the number of spatial channels and/or by employing different modulation formats. The choice of modulation format is limited to dual-polarization (DP) – BPSK, QPSK, 8QAM and 16QAM, with maximum transmission reach calculated by means of the Gaussian Noise (GN) model of nonlinear interference in coherent (Nyquist) WDM systems proposed in [51]. The obtained reach values are presented in Table III.

V. Performance Evaluations and Cost Analysis

In this section, we first compare the performance of spatial Sp-Ch switching paradigms under different spatial and spectral granularities in a network planning scenario for the Telefónica Spain national network. We assume bundles of 12 SMFs with 4.8 THz available spectrum per fiber across all links as a near-term SDM solution. The performance evaluation is done in terms of load and its growth. Since there is a fixed number of demands in the traffic matrix (84 demands), traffic growth is achieved by increasing the size of the demands. In order to perform the studies, we scale the *load* (i.e. total offered load to

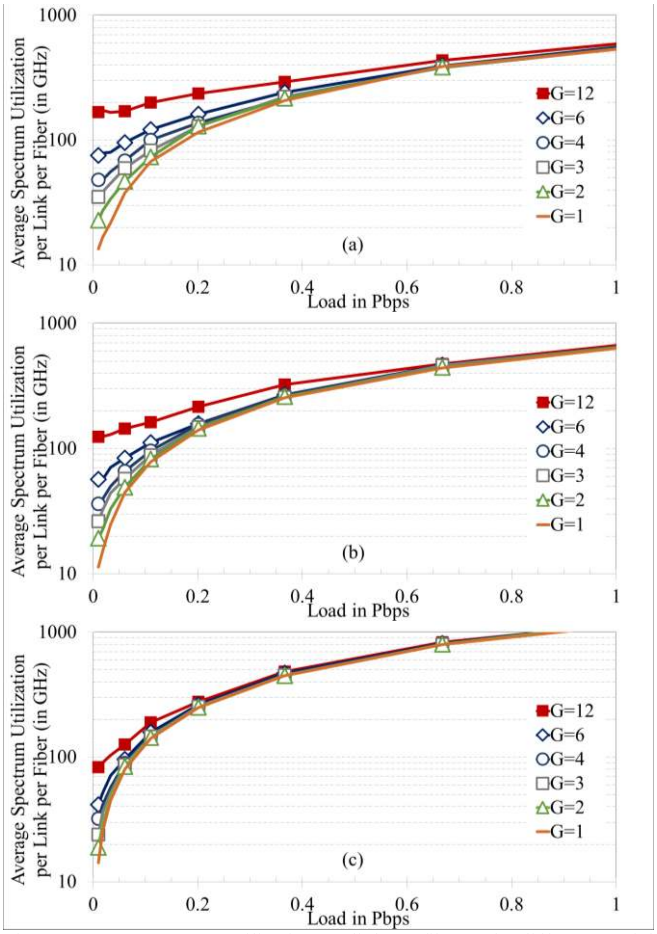

Fig. 4. Average spectrum utilization per link per fiber under different spatial Sp-Ch switching paradigms considering current WSS technology for (a) 50 GHz, (b) 37.5 GHz, and (c) 25 GHz ChBWs at a baud rate of 32, 19.5 and 7 Gbaud, respectively in terms of load.

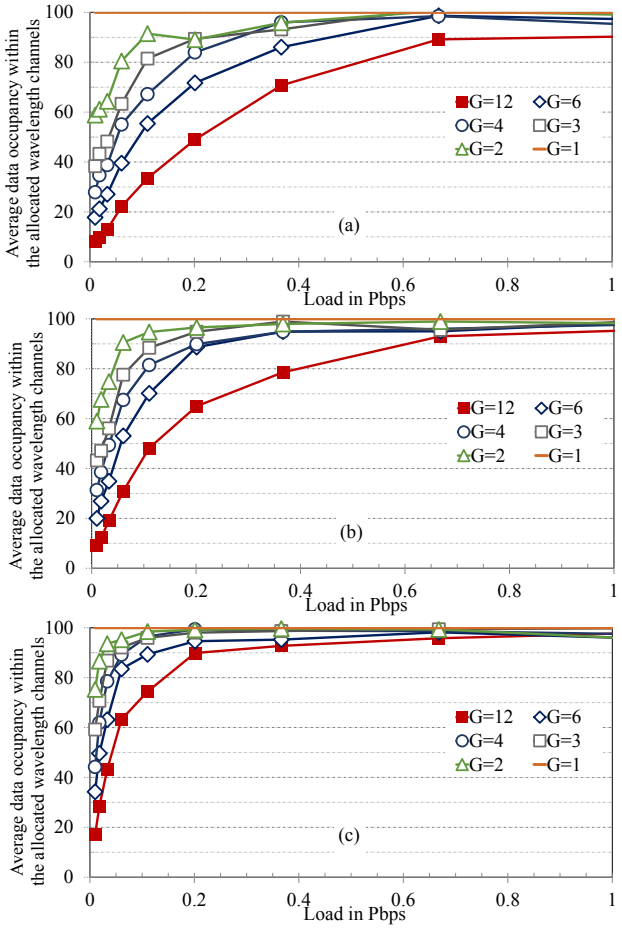

Fig. 5. Average data occupancy in percentage considering current WSS technology for (a) 50 GHz, (b) 37.5 GHz, and (c) 25 GHz ChBWs at a baud rate of 32, 19.5 and 7 Gbaud, respectively in terms of load.

the network) up to 1 Pbps, which is equivalent to 10-year total traffic growth, assuming 45% annual traffic increase. For the spatial switching granularity, we consider groups (G) of 1, 2, 3, 4, 6 and 12 fibers out of 12 fibers in the bundle of SMFs, where G = 1 and 12 correspond to the cases of Ind-Sw and J-Sw, respectively, which offer the finest (Ind-Sw) and the coarsest (J-Sw) spatial granularities. Intermediate values represent FrJ-Sw with spatial groups formed of 2-6 SMFs.

Fig. 4 shows the results considering present-day WSS technology requiring 18 GHz guard band. Fig. 4(a) presents the results for the case of fixed-grid 50 GHz WDM ChBW, in which 32 Gbaud is selected for the contents of each ChBW as it is the maximum baud rate supported by present-day WSS resolution. The average spectrum utilization per link per fiber is used as a quantitative network performance metric. Thus, for example, J-Sw with the coarsest granularity in our studies corresponds to G = 12 and ChBW = 50 GHz, allows for 32GHz×12=384 GHz for data loading, corresponding to 3072 Gb/s assuming DP-16QAM format. Note that, DP-16QAM is the most used modulation format, as most of the lightpaths in the Telefónica network can be established within its optical reach limit. Demands smaller than that will simply occupy the whole spatial-spectral slot, resulting in low data occupancy within the available bandwidth. At the finest granularity of G = 1 and ChBW = 50 GHz, the equivalent minimum spatial-spectral bandwidth slot amounts to 256 Gb/s.

In Fig. 4(a), Ind-Sw shows the best performance for all loads, i.e, lowest utilization for the given traffic load, since it offers the finest granularity. We use it as the benchmark to estimate the unutilized bandwidth due to grouping of spatial dimensions. The performance of the rest of spatial Sp-Ch switching paradigms is seen to converge to that of Ind-Sw as load increases. This is due to the fact that when the load increases the spectral-spatial slot becomes comparable to the demand that has to be served and therefore the amount of unutilized bandwidth due to SG-Sw reduces. Additionally, we observe that, independently of the load, but more noticeably for smaller loads, the curves for the SG-Sw cases with lower values of G (i.e. finer spatial granularity) are closer to the Ind-Sw curve. This is a consequence of the higher flexibility that SG-Sw with low G offers to allocate smaller demands in the space dimension. However, as we will see in the next section, finer spatial granularity results in higher switching infrastructure cost. Current WSS technology with 6.25-GHz assignable spectral slots enables the switching of smaller ChBWs, which allows us to evaluate the impact of spectral switching granularity on the performance of spatial switching paradigms. To carry out this investigation, we repeated the above simulations for 37.5-GHz ChBW at a baud rate of 19.5 Gbaud (Fig. 4(b)), and 25-GHz ChBW at 7 Gbaud (Fig. 4(c)). As observed in Fig. 4(b) and (c), for small values of load, all curves show improved performance compared to the 50-GHz ChBW case since finer data loads can be accommodated per channel.

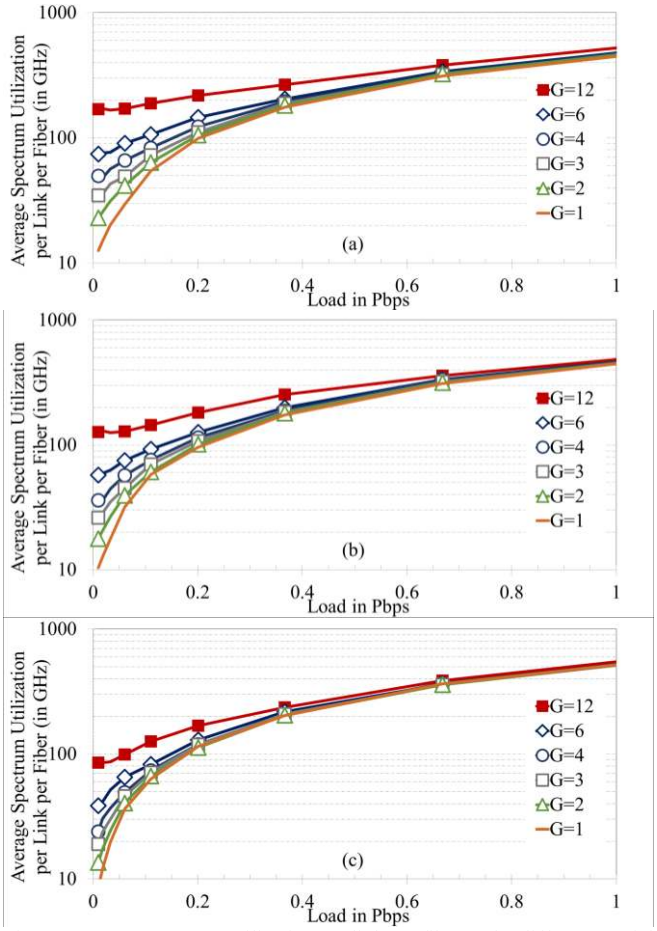

Fig. 6. Average spectrum utilization per link per fiber under different spatial Sp-Ch switching paradigms considering improved resolution WSS technology for (a) 50 GHz, (b) 37.5 GHz, and (c) 25 GHz ChBWs at a baud rate of 41, 28.5 and 16 Gbaud, respectively in terms of load.

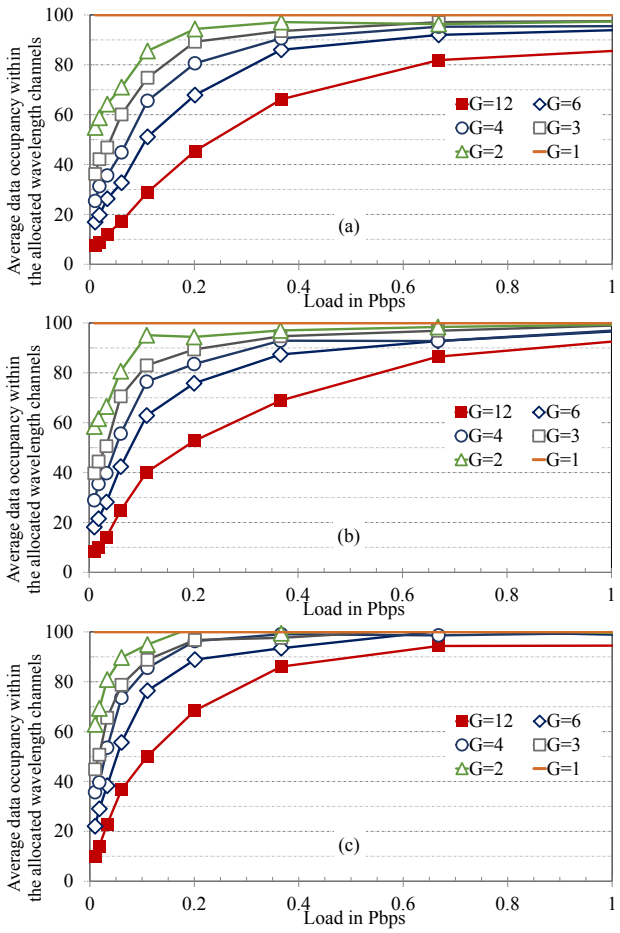

Fig. 7. Average data occupancy in percentage considering finer resolution WSS technology for (a) 50 GHz, (b) 37.5 GHz, and (c) 25 GHz ChBWs at a baud rate of 41, 28.5 and 16 Gbaud, respectively in terms of load.

It is noteworthy that the performance of J-Sw (switching paradigm with the coarsest spatial granularity) converges to that of Ind-Sw for smaller load values, as the ChBW decreases, compared to the case of 50-GHz ChBW. Yet for high loads the spectrum utilization is higher for the case of finer DWDM channel grid, as the finite channel guard bands exhibit lower spectral utilization and more channels have to be provisioned to carry the data.

Another way to quantify the impact of the switching group size is to consider the average 'data occupancy' within an allocated wavelength channel. The data occupancy metric is defined by the bandwidth required to support the data (i.e. equivalent to the baud rate yet measured in GHz) divided by the available bandwidth for data (which is the clear channel bandwidth multiplied by the group size). Ind-Sw always satisfies 100% data occupancy, whereas J-Sw will have the lowest data occupancy (as low as 1/G). As shown in Fig. 5, the amount of data occupancy increases for switching paradigms with finer spatial and/or spectral granularity. Additionally, inflection points in the performance of SG-Sw cases are observed at loads of 0.2 and 0.7 Pb/s, respectively, from where the data occupancy of SG-Sw cases increases significantly. In particular, as observed in Fig. 5(b), the data occupancy in the case of J-Sw goes above 90% for loads higher than ~0.65 Pb/s with 37.5 GHz ChBW, instead of for loads above ~1 Pb/s with 50 GHz ChBW. Finally, Fig. 5(c) shows a further improvement of the performance of different SG-Sw paradigms in comparison with the previous two cases (e.g. the data occupancy of J-Sw increases up to 90% at ~0.2 Pb/s).

Therefore, we can conclude that, for small load values, the utilization of WSSs with finer spectral switching granularity can compensate for the spatial granularity rigidity of SG-Sws. For larger load values, on the other hand, the performance of all switching paradigms is degraded (i.e. the average spectrum utilization increases) as ChBW is decreased. This is due to a less efficient utilization of the spectrum arising from a lower amount of occupied spectrum containing actual traffic compared to the required guard band for the WSSs (i.e. 32/50=64% vs. 7/25=28% for ChBW equal to 50 and 25 GHz, respectively).

In order to evaluate the improvement of the SG-Sw performance resulting from the utilization of WSSs with improved resolution, we repeat the above studies for a WSS technology with a factor-two resolution improvement (i.e. requiring a 9-GHz guard band instead of the 18 GHz considered previously). Fig. 6 attest that the performance of spatial Sp-Ch switching paradigms can be improved by using spatial switches with finer spatial granularity. Likewise, similar to Fig. 4, the use of smaller ChBWs results in performance improvement. Note that, comparing Fig. 6 with Fig. 4, due to the lower guard band required by the WSS with finer resolution, the performance of switching paradigms is not degraded for large load values, in contrast to the case of current WSS technology

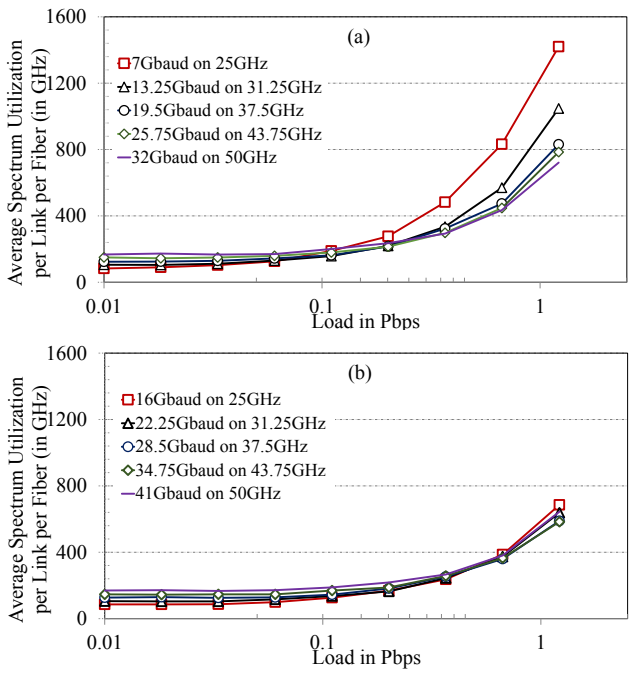

Fig. 8. Average spectrum utilization per link per fiber for J-Sw considering: (a) the current WSS technology which requires 18 GHz for guard band and (b) finer resolution WSS which requires 9 GHz for guard band. Five values of ChBWs are assumed for the simulations. The amount of spectral contents that can be utilized considering different WSS technologies is provided in Table I.

with coarser resolution. However, by comparing Fig. 7 with Fig. 5, we observe that the amount of data occupancy is less significant when the improved resolution WSSs are in place. This is due to the fact that one spectral-spatial slot can accommodate more traffic when WSS technology with factor-two resolution improvement is in place compared to the case of present-day WSS technology. For example, assuming ChBW equal to 50 GHz and DP-16QAM, the capacity of one spatial-spectral is 72 Gb/s higher (i.e. 328 Gb/s – 256 Gb/s) in the case of improved resolution WSS compared to the current WSS technology. Note that, even though the data occupancy (which is a normalized metric) is lower for WSSs with finer spectral resolution, refining the WSS spectral resolution results in a globally better performance, as is shown in Fig. 8.

Fig. 8 presents the results of a more detailed performance evaluation of SG-Sw paradigms for the values of ChBWs indicated in Table I and for two WSS technologies with coarser and finer resolutions. For the sake of clarity, the results are only shown for J-Sw. Fig. 8(a) shows the average spectrum utilization with the current WSS technology. For small loads (<80 Tb/s), as shown previously, smaller ChBW values lead to better J-Sw performance. However, as traffic increases, smaller ChBW values result in significant performance degradation. Fig. 8(b) shows the results when the finer resolution WSS is used. Due to the more efficient utilization of the optical spectrum, smaller ChBW values lead to better performance for loads lower than 800 Tb/s. Even if the performance of J-Sw with smaller values of ChBW reduces for loads larger than 800 Tb/s, this is remarkably better than in the case of WSSs with coarser resolution. Another important finding is that, for small and large loads, the best J-Sw performance is obtained for the lowest and highest values of ChBWs, respectively. Consequently, ChBW must be adaptable to the load level in order to achieve a globally optimum spectrum utilization in an SDM network. This highlights the importance of utilizing flex-grid transmission enabled by spectrally flexible ROADMs and bandwidth variable transceivers when SG-Sw paradigms are considered. A thorough investigation of the benefits/drawbacks of spectrally flex-grid technologies will be the subject of a dedicated study.

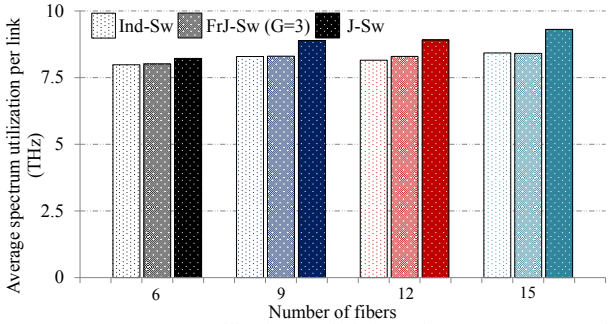

Fig. 9. Average spectrum utilization per link for Ind, FrJ-Sw ($G = 3$), and J-Sw, considering different numbers of fibers for load equal to 1.25Pbps.

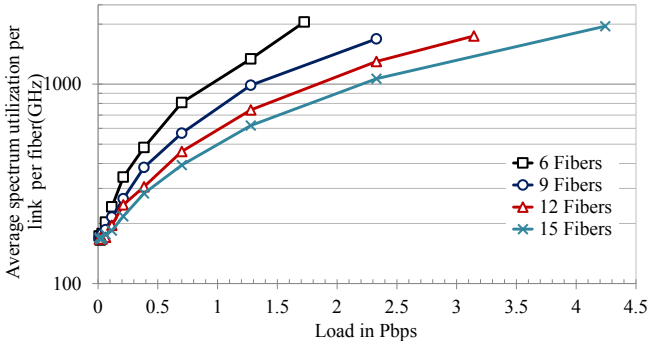

Fig. 10. Average spectrum utilization per link per fiber for different number of fibers in a bundle of fiber with J-Sw in terms of load.

TABLE IV
TOTAL RELATIVE SWITCHING COST OF TELEFÓNICA NETWORK ASSUMING BUNDLES OF 12 SMFS FOR DIFFERENT SWITCHING PARADIGMS CONSIDERING CURRENT WSSS AND IMPROVED RESOLUTION WSSS

Switching Paradigm	Ind-Sw $G = 1$	FrJ-Sw $G = 2$	FrJ-Sw $G = 3$	FrJ-Sw $G = 4$	FrJ-Sw $G = 6$	J-Sw $G = S$
Current WSSs	1693.4	1552.8	1415.7	1227.4	1120	884.8
Improved resolution WSSs	2116.8	1941	1769.6	1534.2	1400	1106

As another contribution of this study, we assess the generality of the above results by exploring the impact of changing the number of SMFs (i.e. S) in the fiber bundles across all links in the network (which also implies adjusting the size of the spatial Sp-Chs accordingly). In Fig. 9, we show the average spectrum utilization per link (differently than Fig. 5 and Fig. 7, which show spectrum utilization per link per fiber) as a function of the number of fibers (we consider bundles of 6, 9, 12 and 15 SMFs) for an exemplary load of 1.25 Pbps. Only G equal to 1, 3 and S are shown for clarity. Likewise, in Fig. 10 the performance of J-Sw in terms of load is plotted for all cases under study. Note that, only the results for ChBW equal to 50 GHz utilizing present-day WSSs are included in Fig. 9 and Fig. 10. All curves follow the same trend as the case of 12 SMFs, which confirms our claim that the performance of all spatial Sp-Ch switching paradigms converge as the load increases. We observe that, by taking advantage of larger spatial Sp-Chs (i.e. higher number of SMFs per bundle per link), more traffic can be accommodated in the network, which translates into longer network serviceability. However, it is important to highlight that the total amount of possible offered load to the network is

affected by the network topology, the heterogeneity of traffic profile, and the location of hot links.

Finally, for a network based on bundles of 12 SMFs, we evaluate the cost of the switching infrastructure for different spatial granularities according to the WSS cost model explained in Section III. As shown in Table IV, our results indicate that Ind-Sw is by far the most expensive solution. Cost savings ranging from 39% to 52%, regardless of the WSS technology, can be achieved with SG-Sw. Switching infrastructures based on improved resolution WSSs show ~25% cost increase in comparison with current WSSs. However, the significant performance improvement, as shown in Fig. 5, which can be translated into longer network serviceability by accommodating much more traffic may be able to justify the 25% increase in the implementation cost.

Considering the results presented in Fig. 4 and Fig. 6 for a single ChBW (e.g. 50 GHz), and assuming the cases of WSS technologies with coarser and finer resolutions, FrJ-Sw with $G = 4$ (for $S = 12$) is the best compromise between network performance and switching-related infrastructure cost. However, if the spectral granularity is allowed to vary, we can observe from Fig. 4 and Fig. 6 that the performance of J-Sw can be improved for loads above a certain threshold. In this situation, even though FrJ-Sw still shows a minimally better performance than J-Sw in terms of spectral occupancy, J-Sw is a more cost-effective solution, and we expect that a network based on J-Sw, due to the possibility of reduced transceiver cost (coming from the use of joint DSP chips common for all spatial sub-channels and the use of a common laser), should lead to even higher overall cost savings in SDM networks, inasmuch as the network CAPEX is dominated by the transceiver cost [29].

VI. Conclusion

In this paper, we compared the performance of different SDM switching paradigms, in terms of spectral occupancy and switching-related infrastructure cost, under various practically feasible spatial and spectral switching granularities as well as considering the current WSS realization and an improved resolution WSS technology over a network based on bundles of SMFs. The network-level simulation results showed that the performance of all switching paradigms converges as traffic increases while the switching-related infrastructure cost can be reduced up to 52% in the SG-Sw cases. Additionally, it was shown that, considering the current WSS technology, the utilization of finer spectral switching granularity significantly improves the performance of SG-Sw paradigms for small values of traffic, which correspond to small demands in the traffic matrix. However, as the load increases, the performance of all switching paradigms reduces due to the less efficient utilization of spectrum arising from a lower amount of occupied spectrum containing actual traffic compared to the required guard band for the WSSs. We also showed that, by utilizing WSSs with improved resolution which require 50% less guard band, the performance of switching paradigms in the case of large values of traffic can be improved by a factor of two at the expense of a 25% increase in the switching infrastructure cost. Having said that, it results from our study that, irrespective of the WSS resolution, large values of ChBW are more beneficial for large values of traffic, and consequently spectral switching granularity must be adaptable to the traffic size in order to achieve a globally optimum spectrum utilization in an SDM network, for which spectrally flex-grid ROADMs and bandwidth-variable transceivers are a requirement.

References

[1] P. J. Winzer, D. T. Neilson, "From scaling disparities to integrated parallelism: A decathlon for a decade," J. Lightw. Technol., DOI: 10.1109/JLT.2017.2662082.

[2] P. J. Winzer, "Optical networking beyond WDM," IEEE Photonics J., vol. 4, no. 2, p. 647-651, Apr., 2012.

[3] P. J. Winzer, "Making spatial multiplexing a reality," in Nature Photonics, vol. 8, no. 5, pp. 345-348, May, 2014.

[4] D. M. Marom, M. Blau, "Switching solutions for WDM-SDM optical networks," IEEE Comm. Mag., vol. 53, no. 2, pp. 60-68, Feb. 2015.

[5] D. M. Marom, P. D. Colbourne, A. D'Errico, N. K. Fontaine, Y. Ikuma, R. Proietti, L. Zong, J. M. Rivas-Moscoso, I. Tomkos, "Survey of photonic switching architectures and technologies in support of spatially and spectrally flexible optical networking [Invited]," J. Opt. Commun. Netw., vol. 9, no. 1, pp. 1-26, Jan., 2017.

[6] D. J. Richardson, J. M. Fini, L. E. Nelson, "Space-division multiplexing in optical fibres," Nature Photonics, vol. 7, no. 5, pp. 354-362, May, 2013.

[7] Y. Li, N. Hua, X. Zheng, G. Li, "Capex advantages of few-mode fiber networks" presented at the Opt. Fiber Commun. Conf. Exhib., Los Angeles, CA, USA, Mar. 2015, Paper Th2A.43.

[8] P. M. Krummrich, "Optical amplifiers for multimode/multi core transmission", presented at the Opt. Fiber Commun. Conf. Exhib., Los Angeles, CA, USA, 2012, Paper OW1D.1.

[9] R. Ryf, S. Chandrasekhar, S. Randel, D. T. Neilson, N. K. Fontaine, and M. Feuer, "Physical layer transmission and switching solutions in support of spectrally and spatially flexible optical networks", IEEE Comm. Mag., vol. 53, no. 2, pp. 52-59, Feb. 2015.

[10] Kazuhide Nakajima, Pierre Sillard, David Richardson, Ming-Jun Li, René-Jean Essiambre, and Shoichiro Matsuo, "Transmission media for an SDM-based optical communication system," IEEE Commun. Mag., vol. 53, no. 2, pp. 44-51, Feb. 2015.

[11] K. Saitoh, and S. Matsuo, "Multicore fiber technology", J. Lightw. Technol., vol. 34, pp.55-66, no. 1, 1 Jan. 2016.

[12] T. Mizuno, H. Takara, K. Shibahara, A. Sano, and Y. Miyamoto, "Dense space division multiplexed transmission over multicore and multimode fiber for long-haul transport systems", J. Lightw. Technol., vol. 34, no. 6, pp. 1484-1493, 15 Mar. 2016.

[13] P. Sillard, "Next-generation fibers for space-division-multiplexed transmissions," presented at the 40th Eur. Conf. Exhib. Opt. Commun., 2014, Cannes, France, Paper Tu.4.1.1.

[14] K. P. Ho, J. M. Kahn, J. P. Wilde, "Wavelength-selective switches for mode-division multiplexing: scaling and performance analysis," J. Lightw. Technol., vol. 32, no. 22, Nov., 2014.

[15] B. Shariati, P. S. Khodashenas, J. M. Rivas-Moscoso, S. Ben-Ezra, D. Klonidis, F. Jimenez, L. Velasco, I. Tomkos, "Evaluation of the impact of different SDM switching strategies in a network planning scenario," presented at the Opt. Fiber Commun. Conf. Exhib., Anaheim, CA, USA, Mar. 2016, Paper Tu2H.4.

[16] B. Shariati, D. Klonidis, D. Siracusa, F. Pederzolli, J. M. Rivas-Moscoso, L. Velasco, I. Tomkos, "Impact of traffic profile on the performance of spatial superchannel switching in SDM networks," in the Proc. of the 42th Eur. Conf. Exhib. Opt. Commun., 2016, Dusseldorf, Germany, Paper M.1.F.1.

[17] F. Pederzolli, D. Siracusa, B. Shariati, J. M. Rivas-Moscoso, E. Salvadori, I. Tomkos, "Improving Performance of Spatially Joint- Switched Space Division Multiplexing Optical Networks via Spatial Group Sharing," J. Opt. Commun. Netw., vol. 9, no. 3, pp. B1-B10, Mar., 2017.

[18] B. Shariati, D. Klonidis, J. M. Rivas-Moscoso and I. Tomkos, "Evaluation of the impact of spatial and spectral granularities on the performance of spatial superchannel switching schemes," 18th International Conf. Trans. Opt. Netw. (ICTON), Trento, 2016, Paper Tu.D1.5.

[19] M. D. Feuer, "Optical routing for SDM networks," presented at the Eur. Conf. Opt. Commun., Valencia, Spain, 2015, Paper Th.2.5.5.

[20] D. Klonidis, F. Cugini, O. Gerstel, M. Jinno, V. Lopez, E. Palkopoulou, M. Sekiya, D. Siracusa, G. Thouénon, and C. Betoule, "Spectrally and

spatially flexible optical network planning and operations," IEEE Commun. Mag., vol. 53, no. 2, pp. 69-78, Feb., 2015.

[21] P. S. Khodashenas, J. M. Rivas-Moscoso, D. Siracusa, F. Pederzolli, B. Shariati, D. Klonidis, E. Salvadori, and I. Tomkos, "Comparison of spectral and spatial super-channel allocation schemes for SDM networks", J. Lightw. Technol., vol. 34, no. 11, pp. 2710-2716, June 2016.

[22] S. Ö. Arik, K-P Ho, and J. M. Kahn, "Optical network scaling: roles of spectral and spatial aggregation," in Proc. SPIE 9389, Next-Generation Optical Communication: Components, Sub-Systems, and Systems IV, 93890B (2015).

[23] A. Muhammad, G. Zervas, D. Simeonidou and R. Forchheimer, "Routing, spectrum and core allocation in flexgrid SDM networks with multi-core fibers," presented at International Conference on Optical Network Design and Modeling, 2014, Stockholm, Sweden, pp. 192-197.

[24] A. Muhammad, G. Zervas, and R. Forchheimer, "Resource allocation for space-division multiplexing: optical white box versus optical black box networking", J. Lightw. Technol., vol. 33, no. 23, pp. 4928-4941, 2015.

[25] H. Tode, Y. Hirota, "Routing, spectrum, and core and/or mode assignment on space-division multiplexing optical networks," J. Opt. Commun. Netw., vol. 9, no. 1, pp. A99-113, Jan., 2017.

[26] C. Rottondi, P. Boffi, P. Martelli, M. Tornatore, "Routing, modulation format, baud rate and spectrum allocation in optical metro rings with flexible grid and few-mode transmission," J. Lightw. Technol., doi: 10.1109/JLT.2016.2627618.

[27] M. D. Feuer, L. E. Nelson, X. Zhou, S. L. Woodward, R. Isaac, B. Zhu, T. F. Taunay, M. Fishteyn, J. M. Fini, and M. F. Yan, "Joint digital signal processing receivers for spatial superchannels", Photon. Technol. Lett., vol. 24, no. 21, pp. 1957-1960, 1 Nov. 2012.

[28] L. E. Nelson, M. D. Feuer, K. Abedin, X. Zhou, T. F. Taunay, J. M. Fini, B. Zhu, R. Isaac, R. Harel, G. Cohen, D. M. Marom, "Spatial superchannel routing in a two-Span ROADM system for space division multiplexing," J. Lightw. Technol., vol. 32, no. 4, pp. 783–789, Feb., 2014.

[29] J. M. Rivas-Moscoso, B. Shariati, A. Mastropaolo, D. Klonidis, I. Tomkos, "Cost benefit quantification of SDM network implementations based on spatially integrated network elements," presented at the 42th Eur. Conf. Exhib. Opt. Commun., 2016, Dusseldorf, Germany, Paper M1.5.4.

[30] T. Watanabe, K. Suzuki, T. Goh, K. Hattori, A. Mori, T. Takahashi, T. Sakamoto, K. Morita, S. Sohma, and S. Kamei, "Compact PLC-based Transponder Aggregator for Colorless and Directionless ROADM," presented at the Opt. Fiber Commun. Conf. Exhib., Los Angeles, CA, USA, Mar. 2011, Paper OTuD3.

[31] Leonid Pascar, Reuven Karubi, Boris Frenkel, and Dan M. Marom, "Port-Reconfigurable, Wavelength-Selective Switch Array for Colorless/Directionless/Contentionless Optical Add/Drop Multiplexing", presented at Photonics in Switching 2015, Florence (Italy), pp. 301-303, paper PDP.2.

[32] Y. Ikuma, K. Suzuki, N. Nemoto, E. Hashimoto, O. Moriwaki, and T. Takahashi, "8 × 24 Wavelength Selective Switch for Low-loss Transponder Aggregator," presented at the Opt. Fiber Commun. Conf. Exhib., Los Angeles, CA, USA, Mar. 2015, Paper Th5A.4.

[33] Y. Ikuma, K. Suzuki, N. Nemoto, E. Hashimoto, O. Moriwaki and T. Takahashi, "Low-Loss Transponder Aggregator Using Spatial and Planar Optical Circuit," J. Lightw. Technol., vol. 34, no. 1, pp. 67-72, Jan. 2016.

[34] J. Carpenter, S. G. Leon-Saval, J. R. Salazar-Gil, J. Bland-Hawthorn, G. Baxter, L. Stewart, S. Frisken, M. A. F. Roelens, B. J. Eggleton, and J. Schröder, "1x11 few-mode fiber wavelength selective switch using photonic lanterns," Opt. Express, vol. 22, no. 3, pp. 2216-2221, Jan. 2014.

[35] N. K. Fontaine, T. Haramaty, R. Ryf, H. Chen, L. Miron, Pascar, M. Blau, B. Frenkel, L. Wang, Y. Messaddeq, S. LaRochelle, R. J. Essiambre, Y. Jung, Q. Kang, J. K. Sahu, S. U. Alam, D. J. Richardson, D. M. Marom, "Heterogeneous space-division multiplexing and joint wavelength switching demonstration," presented at the Opt. Fiber Commun. Conf. Exhib., Los Angeles, CA, USA, Mar., 2015, Paper Th5C.5.

[36] K. Suzuki, Y. Ikuma, E. Hashimoto, K. Yamaguchi, M. Itoh, and T. Takahashi, "Ultra-High Port Count Wavelength Selective Switch Employing Waveguide-Based I/O Frontend", presented at the Opt. Fiber Commun. Conf. Exhib., Los Angeles, CA, USA, Mar., 2015, Paper Tu3A.7.

[37] K. Suzuki, M. Nakajima, K. Yamaguchi, G. Takashi, Y. Ikuma, K. Shikama, Y. Ishii, M. Itoh, M. Fukutoku, T. Hashimoto, and Y. Miyamoto, "Wavelength selective switch for multi-core fiber based space division multiplexed network with core-by-core switching capability," in Photonics Switching (PS), Niigata, Japan, July 2016.

[38] M. Jinno and Y. Mori, "Unified Architecture and Design Methodology for Integrated SDM-WSS Employing PLC-Based Spatial Beam Transformer Array for Various Types of SDM Fibers," presented at the Opt. Fiber Commun. Conf. Exhib., Anaheim, CA, USA, Mar. 2016, Paper W4B.3.

[39] Bin Huang, Nicolas K. Fontaine, Roland Ryf, Binbin Guan, Sergio G. Leon-Saval, R. Shubochkin, Y. Sun, R. Lingle, and Guifang Li, "All-fiber mode-group-selective photonic lantern using graded-index multimode fibers," Opt. Express, vol. 23, no. 1, pp. 224-234, Jan. 2015.

[40] P. Mitchell, G. Brown, R. Thomson, N. Psaila and A. Kar, "57 channel (19×3) spatial multiplexer fabricated using direct laser inscription," presented at the Opt. Fiber Commun. Conf. Exhib., San Francisco, CA, USA, Mar. 2014, Paper M3K.5.

[41] Z. Sanjabi Eznaveh, J.E. Antonio Lopez, G. Lopez Galmiche, J. Rodriguez Asomoza, D. Van Ras, P. Sillard, A. Schülzgen, C. M. Okonkwo, and R. Amezcua Correa, "Few Mode Multicore Photonic Lantern Multiplexer, " presented at the Opt. Fiber Commun. Conf. Exhib., Los Angeles, CA, USA, Mar. 2016, Paper Tu3I.5.

[42] R. R. Thomson, H. T. Bookey, N. D. Psaila, A. Fender, S. Campbell, W. N. MacPherson, J. S. Barton, D. T. Reid, and A. K. Kar, "Ultrafast-laser inscription of a three dimensional fan-out device for multicore fiber coupling applications," Opt. Exp., vol. 15, no. 18, pp. 11691-11697, Sep. 2007.

[43] B. Zhu, T. F. Taunay, M. F. Yan, J. M. Fini, M. Fishteyn, E. M. Monberg, and F. V. Dimarcello, "Seven-core multicore fiber transmissions for passive optical network," Opt. Exp., vol. 18, no. 11, pp. 11117-11122, 24 May 2010.

[44] D. M. Marom, J. Dunayevsky, D. Sinefeld, M. Blau, R. Ryf, N. K. Fontaine, M. Monloadiu, S. Randel, C. Liu, B. Ercan, M. Esmaeelpour, S. Chandrasekhar, A. H. Gnauck, S. G. Leon-Saval, J. Bland-Hawthorn, J. R. Salazar-Gil, Y. Sun, L. Grüner-Nielsen, R. Lingle, "Wavelength-selective switch with direct few mode fiber integration," in Optics Express, vol. 23, no. 5, p. 5723-5737, Feb., 2015.

[45] R. Y. Gu, E. Ip, M.-J. Li, Y.-K. Huang, and J. M. Kahn, "Experimental demonstration of a spatial light modulator-based few-mode fiber switch for space-division multiplexing," presented at Frontiers Opt., 2013, Orlando, FL, USA, Paper FW6B.

[46] N. K. Fontaine, H. Chen, B. Ercan, R. Ryf, G. Labrouille, N. Barré, P. Jian, J. F. Morizur, and D. T. Neilson, "Wavelength Selective Switch with Optimal Steering Element Utilization," presented at the Opt. Fiber Commun. Conf. Exhib., Anaheim, CA, USA, Mar. 2016, Paper Th5A.6.

[47] INSPACE Project website: http://www.ict-inspace.eu/

[48] B. Shariati, P. S. Khodashenas, J. M. Rivas-Moscoso, S. Ben-Ezra, D. Klonidis, F. Jimenez, L. Velasco, I. Tomkos, "Investigation of mid-term network migration scenarios comparing multi-band and multi-fiber deployments", presented at the Opt. Fiber Commun. Conf. Exhib., Anaheim, CA, USA, Mar. 2016, Paper Th1E.1.

[49] T. Eilam-Tzoreff, "The disjoint shortest paths problem," in Elsevier Discrete Applied Mathematics (1998), vol. 85, no. 2, pp.113-138.

[50] K. Christodoulopoulos, I. Tomkos, and E. A. Varvarigos, "Elastic bandwidth allocation in flexbile OFDM-based optical networks", J. Lightw. Technol., vol. 29, no. 9, pp. 1354-1366, Mar., 2011.

[51] E. Palkopoulou, G. Bosco, A. Carena, D. Klonidis, P. Poggiolini, I. Tomkos, "Nyquist-WDM-based flexible optical networks: exploring physical layer design parameters", J. Lightw. Technol., vol. 31, no. 14, pp. 2332-2339, Jul 2013.